Probing the Role of Backbone Hydrogen Bonds in Protein−Peptide Interactions by Amide-to-Ester Mutations

Jonas N. N. Eildal,[†,‡] Greta Hultqvist,[‡] Thomas Balle,[§] Nicolai Stuhr-Hansen,[†] Shahrokh Padrah,[†] Stefano Gianni,[∥] Kristian Strømgaard,*[,†] and Per Jemth*[,‡]

[†]Department of Drug Design and Pharmacology, University of Copenhagen, Universitetsparken 2, DK-2100 Copenhagen, Denmark

[‡]Department of Medical Biochemistry and Microbiology, Uppsala University, BMC Box 582, SE-75123 Uppsala, Sweden

[§]Faculty of Pharmacy, The University of Sydney, Sydney, NSW 2006, Australia

[∥]Department Biochemical Sciences, Sapienza, University of Rome, P.le A. Moro 5, Rome, 00185, Italy

S *Supporting Information*

ABSTRACT: One of the most frequent protein−protein interaction modules in mammalian cells is the postsynaptic density 95/discs large/ zonula occludens 1 (PDZ) domain, involved in scaffolding and signaling and emerging as an important drug target for several diseases. Like many other protein−protein interactions, those of the PDZ domain family involve formation of intermolecular hydrogen bonds: C-termini or internal linear motifs of proteins bind as β-strands to form an extended antiparallel β-sheet with the PDZ domain. Whereas extensive work has focused on the importance of the amino acid side chains of the protein ligand, the role of the backbone hydrogen bonds in the binding reaction is not known. Using amide-to-ester substitutions to perturb the backbone hydrogen-bonding pattern, we have systematically probed putative backbone hydrogen bonds between four different PDZ domains and peptides corresponding to natural protein ligands. Amide-to-ester mutations of the three C-terminal amides of the peptide ligand severely affected the affinity with the PDZ domain, demonstrating that hydrogen bonds contribute significantly to ligand binding (apparent changes in binding energy, $\Delta\Delta G$ = 1.3 to >3.8 kcal mol^{-1}). This decrease in affinity was mainly due to an increase in the dissociation rate constant, but a significant decrease in the association rate constant was found for some amide-to-ester mutations suggesting that native hydrogen bonds have begun to form in the transition state of the binding reaction. This study provides a general framework for studying the role of backbone hydrogen bonds in protein−peptide interactions and for the first time specifically addresses these for PDZ domain−peptide interactions.
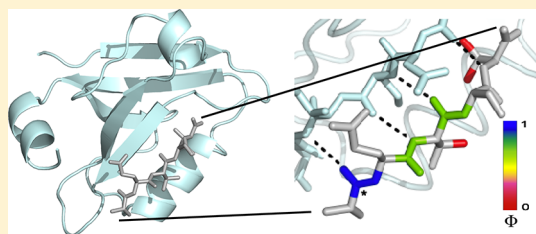
INTRODUCTION

A number of interaction modules govern signaling and scaffolding in mammalian cells. A very important and highly frequent type of interaction module is the one found in the family of postsynaptic density 95 (PSD-95)/discs large/zonula occludens 1 (PDZ) domains,[1−4] which generally recognizes short regions of amino acid sequences, in particular flexible C-termini of target protein ligands (Figure 1A). PDZ domains play important roles in a plethora of physiological functions, for example, acting as scaffolding proteins in the synapse[2,5] and as recognition motifs in enzymes, such as protein tyrosine phosphatase.[6] In each of these interactions, a number of hydrogen bonds are formed between the natural ligand and the PDZ domain. PDZ domains are also emerging as novel and exciting drug targets, based on inhibition of the protein−PDZ domain interaction.[7,8] Currently, the most advanced compounds are those that inhibit PDZ domains of PSD-95 as putative treatment of ischemia and pain.[9−13]

It is well established that the C-terminal part of the protein ligand or an internal linear motif is bound to a peptide binding groove in the PDZ domain, between the β2-strand and the α2-helix (Figure 1A).[14] The ligand forms an extended antiparallel

intermolecular β-sheet with two β-strands from the PDZ domain. In X-ray crystal and NMR structures of PDZ domains together with peptides corresponding to C-termini of putative protein ligands, it is suggested that three or perhaps four hydrogen bonds are formed between the backbone of the ligand and β2 of the PDZ domain (Figure 1A). These structurally conserved hydrogen bonds are likely to contribute to the affinity of the protein ligand-PDZ complex and might be involved in early events during the binding reaction. While numerous studies have evaluated the importance of amino acid side chains in the ligand with respect to affinity and selectivity,[15−23] the role of the backbone hydrogen bonds in these interactions has not been assessed.

One of the best ways to probe backbone interactions is to introduce amide-to-ester mutations, which is a subtle modification that removes the NH hydrogen-bond donor and reduces the hydrogen-bond acceptor capacity of the carbonyl group by ca. 50%.[24] The strategy has been used in protein folding and stability studies,[25−32] amyloid formation,[33] and in
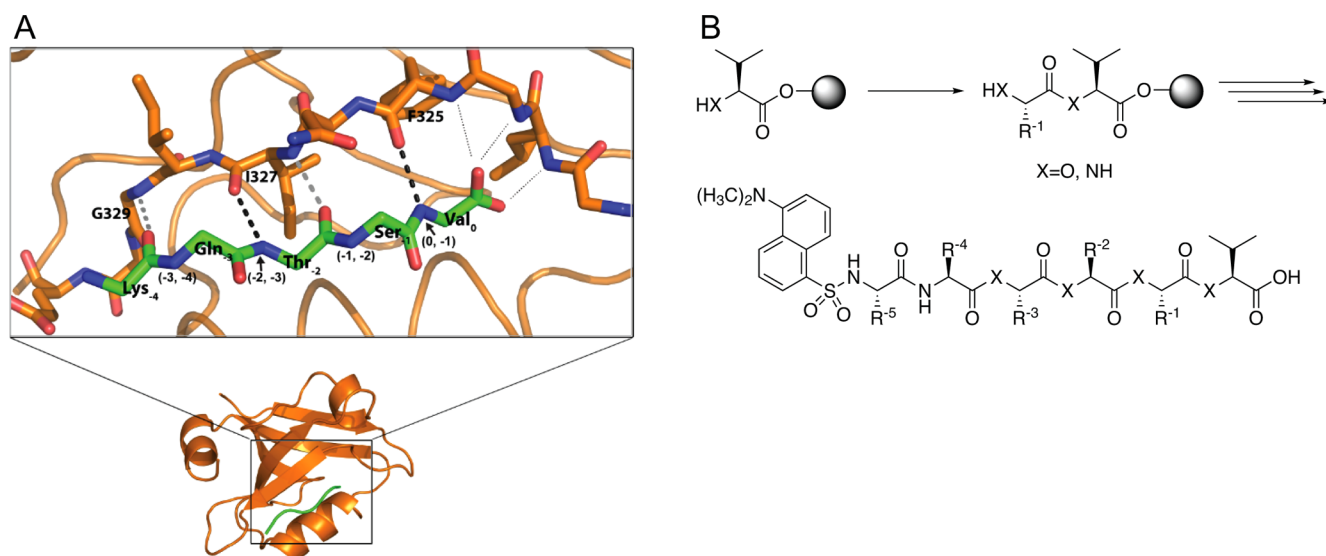
Figure 1. (A) Structure of PSD-95 PDZ3 with bound peptide. Putative hydrogen bonds between the PDZ domain backbone and the peptide ligand are indicated. In the present study we target the hydrogen bonds indicated by large dots by amide-to-ester mutations. Black dots represent hydrogen bonds that are completely deleted by the mutation, whereas gray dots denote hydrogen bonds between a peptide carbonyl and PDZ NH, which are destabilized but not removed by the mutation. The three hydrogen bonds between the peptide carboxylate and the conserved GLGF loop are shown as small dots. Note that peptide ligands of PDZ domains are numbered from 0 (at the C-terminus) and −1, −2, etc. toward the N-terminus. We refer to a particular mutated hydrogen bond as, for example, (0, −1), meaning that the amide NH between residue 0 and −1 has been replaced by an oxygen. (B) General synthesis of dansyl labeled depsipeptides. Hexa-depsipeptides were prepared using either Fmoc- or Boc-based SPPS, and ester bonds were introduced by coupling of α-hydroxy acids. In all cases the N-terminal was derivatized with a dansyl group.

interactions between enzymes and substrates or inhibitors[34−36] as well as in interactions between nicotinic acetylcholine receptor and its ligands.[37,38] Here we have for the first time systematically explored the general importance of backbone hydrogen bonds in protein−peptide interactions involving PDZ domains, using four prototypical PDZ domains and peptides corresponding to naturally occurring protein ligands. There is a severe loss of affinity upon destabilization or removal of several backbone hydrogen bonds, revealing their pivotal role in the PDZ−peptide interaction. Furthermore, we use kinetic methods to probe the role of these hydrogen bonds in the transition state for the binding reaction and find that in some cases their formation is partially rate limiting.

■ METHODS

Synthesis of Depsipeptides. All starting materials were obtained from Sigma-Aldrich or IRIS Biotech. Amino acids, 2-chlorotrityl chloride, preloaded Boc-Val-PAM resin were purchased from either IRIS Biotech or Peptides International. Cy5-maleimide was purchased from GE-Healthcare. All starting materials and solvents were used without further purification except DCM, DMF, and THF which were stored over molecular sieves (3 Å). Further, THF was freshly distilled prior to storage. Analytical high-performance liquid chromatography (HPLC) was performed on an Agilent 1100 system with a C18 reverse phase column (Zorbax 300 SB-C18 column, 4.6 × 150 mm), flow rate of 1 mL/min, and a linear gradient of the binary solvent system of H₂O/MeCN/TFA (A: 95/5/0.1; B: 5/95/0.1). Preparative reverse phase HPLC (RP-HPLC) was performed on a Agilent 1200 system using a C18 reverse phase column (Zorbax 300 SB-C18, 21.2 × 250 mm) with a linear gradient using either of two binary solvent systems: (1) H₂O/MeCN/TFA (A: 95/5/0.1; B: 5/95/0.1) or (2) (A: 0.1 M triethylammonium acetate (pH adjusted to 4.5); B: MeCN), with a flow rate of 20 mL/min. Solvent system (1) was used unless otherwise stated. Mass spectra were obtained with an Agilent 6410 Triple Quadrupole Mass Spectrometer instrument using electron spray ionization (ESI) coupled to an Agilent 1200 HPLC system (ESI-LC/MS) with a C18 reverse phase column (Zorbax Eclipse XBD-C18, 4.6

× 50 mm), autosampler, and diode array detector using a linear gradient of the binary solvent system of H₂O/MeCN/formic acid (A: 95/5/0.1; B: 5/95/0.086) with a flow rate of 1 mL/min. During ESI-LC/MS analysis, evaporative light scattering (ELS) traces were obtained with a Sedere Sedex 85 Light Scattering Detector. High-resolution mass spectra (HRMS) were obtained using an ESI and Micromass Q-Tof 2 instrument and were all within ±5 ppm of theoretical values.

Wild-type dansylated peptides were manually synthesized by an Fmoc-based solid-phase peptide synthesis (SPPS) strategy in a 0.25 mmol scale on a MiniBlock (Mettler-Toledo, OH, U.S.A.) using a preloaded H-L-Val-2-chlorotrityl chloride resin (200−400 mesh). After swelling the resin in dry DCM for 15−30 min, coupling steps were carried out with N-[1H-benzotriazol-1-yl)(dimethylamino)-methylene]-N-methyl-methanaminium hexafluorophosphate N-oxide (HBTU) and diisopropylethylamine (DIPEA) (resin/amino acid/HBTU/DIPEA, 1:4:4:8) in dry DMF (3 mL) for 30 min. Fmoc deprotection steps were carried out with 20% piperidine in DMF (1 × 5 and 1 × 15 min) washing with DMF in between and after. Following the subsequent coupling steps and N-terminal deprotection of the final amino acid, treatment of the resin-bound peptide with dansyl-chloride (4 equiv) and DIPEA (6 equiv) in dry DCM (3 mL) for 1 h, followed by washing with DCM, MeOH, DCM afforded the dansylated hexapeptides. Final cleavage from the resin was performed by treatment with TFA/TIPS/H₂O (95:2.5:2.5) for 2 h followed by evaporation *in vacuo*, cold ether precipitation, lyophilization, and reverse phase HPLC purification. Final peptides were lyophilized affording white or yellowish solids with purities generally >95% (Table S1).

Dansylated depsipeptides at position (0,−1) were manually synthesized as above by a Fmoc-based SPPS strategy starting with a 2-chlorotrityl chloride resin (200−400 mesh, 1% DVB) as a solid support in a 0.25 mmol scale. After swelling the resin in dry DCM for 15−30 min, (S)-(+)-2-hydroxy-3-methylbutyric acid (4 equiv) was dissolved in dry DCM (3 mL) and added to the resin with DIPEA (8 equiv), subsequently agitating for 1 h followed by washing of the resin with DCM and DMF. The ester bond forming Fmoc protected amino acid (5.6 equiv) was dissolved in 1:1 mixture of DCM/DMF (2.5 mL) on ice and N,N′-diisopropylcarbodiimide (DIC) (5 equiv) was added.

After 15 min the mixture was added to the resin followed by addition of 4-dimethylaminopyridine (DMAP) (0.1 equiv) and *N*-ethyl-morpholine (NEM) (2 equiv) agitating for 1 h at room temperature. After washing the resin with DCM and then DMF, this coupling step was repeated. Subsequent Fmoc deprotection and coupling steps as well as N-terminal dansylation was carried out as described for wild-type peptides above. The final peptides were cleaved from the resin by treatment with TFA/TIPS/H$_2$O (95:2.5:2.5) for 2 h and treated as the wild-type peptides described above, yielding the purified (0,−1) dansylated depsipeptides as white or yellowish solids after lyophilization with purities generally >95% (Table S1).

Despsipeptides with mutations at (−1,−2), (−2,−3) and (−3,−4) were synthesized by a Boc-based SPPS strategy starting with a preloaded Boc-Val-PAM resin (200−400 mesh) in a 0.125−0.25 mmol scale. After swelling the resin in dry DCM for 15−30 min, Boc deprotection of the preloaded amino acid was carried out in neat TFA (2 × 1 min) followed by washes with DCM and DMF. Coupling of α-hydroxy acids was carried out by dissolving the α-hydroxy acid (5.6 equiv) in a 1:1 mixture of DCM/DMF (2.5 mL) on ice followed by addition of DIC (5 equiv) and hydroxybenzotriazole (HOBt) (6 equiv). After 15 min the mixture was added to the resin along with NEM (2 equiv) followed by agitating for 10 min at room temperature and washing steps with DMF and DCM. Ester bond formation was achieved by dissolving the subsequent Boc-protected amino acid (5.6 equiv) in a mixture of 1:1 DCM/DMF (2.5 mL) on ice and adding DIC (5 equiv). After 15 min the mixture was added to the resin followed by addition of DMAP (0.1 equiv) and NEM (2 equiv) agitating for 1 h at room temperature. Following washes with DCM and DMF this coupling step was repeated. Subsequent Boc deprotections were carried out with neat TFA (2 × 1 min) followed by washes with DCM and DMF. Standard coupling and dansylation steps were carried out as for wild-type peptides described above. The final cleavage of the peptides was achieved by treating the resin with anhydrous HF/*p*-cresol (9:1, v/v) or anhydrous HF/*p*-cresol/*p*-thiocresol (9:0.5:0.5, v/v) for peptides containing arginine, for 2 h at 0 °C. The crude products were precipitated with cold ether, lyophilized, and purified by reverse phase HPLC, affording the final depsipeptides as white or yellowish solids with purities generally >95%. Characterization and final purity of all peptides was determined by HPLC, LC-MS, and HRMS (Table S1).

Expression and Purification of PDZ Domains. Expression and purification of PSD-95 PDZ2,[39] PSD-95 PDZ3,[40] SAP97 PDZ2,[41] and PTP-BL PDZ2[42] were performed as previously described. The concentration of PDZ domains was estimated from the absorbance at 280 nm and the calculated extinction coefficients. The amino acid sequences of the constructs and positions of engineered Trp residues were described by Chi et al.[39,41]

Fluorescence Polarization Measurements. For measuring the binding affinity between depsipeptides and PDZ domains, saturation-binding experiments were first performed between the four PDZ proteins PSD-95 PDZ2, PSD-95 PDZ3, SAP-97 PDZ2, and PTP-BL PDZ2 and their corresponding four Cy5-labeled peptides (denoted probes): N2B (CSGYEKLSSIESDV), CRIPT (CNNGLDTKNYKQTSV), Nav1.4 (CNNGVRPGVKESLV), and TRPV3 (CNNGELDEFPETSV), respectively. The PDZ domain was added at increasing concentration, to a fixed concentration of the probe (50 nM) to get a saturation-binding curve. The assay was performed in 150 mM NaCl, 10 mM Tris, pH 7.4, including 1% BSA in black flat bottom 384-well plates (Corning Life Sciences, NY) at 25 °C as described.[20,43] Next, to measure the affinities between dansylated wild-type and depsipeptides and their respective PDZ domains, heterologous competition binding experiments were performed by adding increasing concentration of depsipeptide to a fixed concentration of Cy5-labeled probe (25−50 nM) and PDZ protein (2.5−5 μM) under the same conditions as described above. FP values were then fitted to the equation: $Y = \text{bottom} + (\text{top} - \text{bottom})/(1 + 10^{(X - \log \text{IC}_{50})})$, where X is the logarithmic value of peptide concentration and IC$_{50}$ is the concentration giving half saturation. The IC$_{50}$ values were then used to calculate the inhibition dissociation constants, K_i.[43]

Binding Kinetics. Kinetic experiments were performed in 50 mM potassium phosphate, pH 7.5, 100 mM NaCl at 10 °C, on an upgraded SX-17 stopped flow spectrometer from Applied Photophysics (Leatherhead, U.K.) by mixing PDZ domain with different concentrations of peptide and monitoring the change in Trp or dansyl fluorescence. Excitation was at 290 nm, and emission was recorded at 330 ± 30 nm using a band-pass filter. The concentrations of depsipeptides were determined by the absorbance of the dansyl group at 330 nm. Final concentrations of the PDZ domains were: 3 μM for PSD-95 PDZ2, SAP97 PDZ2, and PTP-BL PDZ2 and 5 μM for PSD-95 PDZ3. Each kinetic trace was fitted to a single exponential function, and the resulting k_{obs} value was plotted versus peptide concentration and analyzed as described[23,44] to obtain the kinetic parameter k_{on}. The k_{off} values were either derived directly from curve fitting of binding data (PSD-95 PDZ2 and PTP-BL PDZ2) using an equation derived for a second-order bimolecular binding reaction[44] or measured by performing displacement experiments (PSD-95 PDZ3 and SAP97 PDZ2). In such displacement experiments, the PDZ (1 μM) in complex with dansylated wild-type or depsipeptide (5 μM) was mixed rapidly with unlabeled ligand (0−80 μM), and k_{off} determined as the extrapolated rate constant at high concentration of unlabeled native peptide ligand.[23] Temperature jump experiments were performed on a joule heating (capacitor discharge) instrument (TgK Scientific, Bradford-on-Avon, U.K.) for PTP-BL PDZ2. The concentration of PTP-BL PDZ2 was 10 μM with concentrations of 50, 200, and 400 μM peptide ligand, respectively. $\Phi_{binding}$[45] was defined as $\Delta\Delta G_{TS}/\Delta\Delta G_{Eq}$, where $\Delta\Delta G_{TS} = RT \ln (k_{on}^{mutant}/k_{on}^{wild-type})$ and $\Delta\Delta G_{Eq} = RT \ln (K_d^{wild-type}/K_d^{mutant})$. K_d values were obtained from the ratio of k_{off} and k_{on}, except for PSD-95 PDZ3, positions (−1,−2) and (−2,−3), where $\Delta\Delta G_{Eq}$ values were estimated from K_i values from fluorescence polarization experiments.

Computational Methods. Relaxed torsional scans were performed around the peptide backbone (N−Cα and Cα−CO) for an AQTSV model peptide derived from the WT KQTSV peptide ligand cocrystallized with PSD-95 PDZ3 (PDB entry: 1BE9)[14] and the corresponding depsipeptides. The calculations were performed in steps of 5° in MacroModel 9.9 (Schrödinger, LLC, New York, 2011) using the OPLS2005 force field[46] and the GB/SA solvation model.[47] The model peptide which contains an alanine in place of the lysine was used to avoid introducing bias from the lysine side chain which is undefined in the X-ray structure. For the same reason, computational studies were restricted to exploring (0,−1), (−1,−2) and (−2,−3) depsipeptides and the wild-type peptide with amide bonds. The relative conformational energies are plotted against the dihedral angle in Figure S1. The molecular mechanics calculations provide a qualitative measure for the change in conformational preferences as a function of the introduced amide-to-ester mutations. To quantify the effect, relaxed backbone coordinate scans were performed for Val−CO−CH$_3$ and the corresponding depsifragment using quantum mechanical (QM) calculations in Jaguar 7.8 (Schrödinger, LLC, New York, 2011). The scan was performed in steps of 10° using the B3LYP/6-31+G** functional[48,49] and basis set with the Poisson−Boltzmann aqueous solvation model.[50] Otherwise default settings were used. Gas-phase energies were extracted and plotted against dihedral angle (Figure S2).

■ RESULTS

To address the role of backbone hydrogen bonds in PDZ−peptide interactions, we selected four PDZ domains: PDZ2 and PDZ3 of PSD-95, PDZ2 of synapse-associated protein 97 (SAP97), and PDZ2 of protein tyrosine phosphatase-BL (PTP-BL) and their corresponding hexapeptide binding partners matching naturally occurring protein ligands (SIESDV, YKQTSV, RRETQV, and EQVSAV, respectively). Since five or six C-terminal amino acids in most cases are sufficient to establish wild-type affinities for PDZ−peptide interactions,[20,21] we rationalized that important backbone interactions from the peptide ligands would be found primarily in this part of the
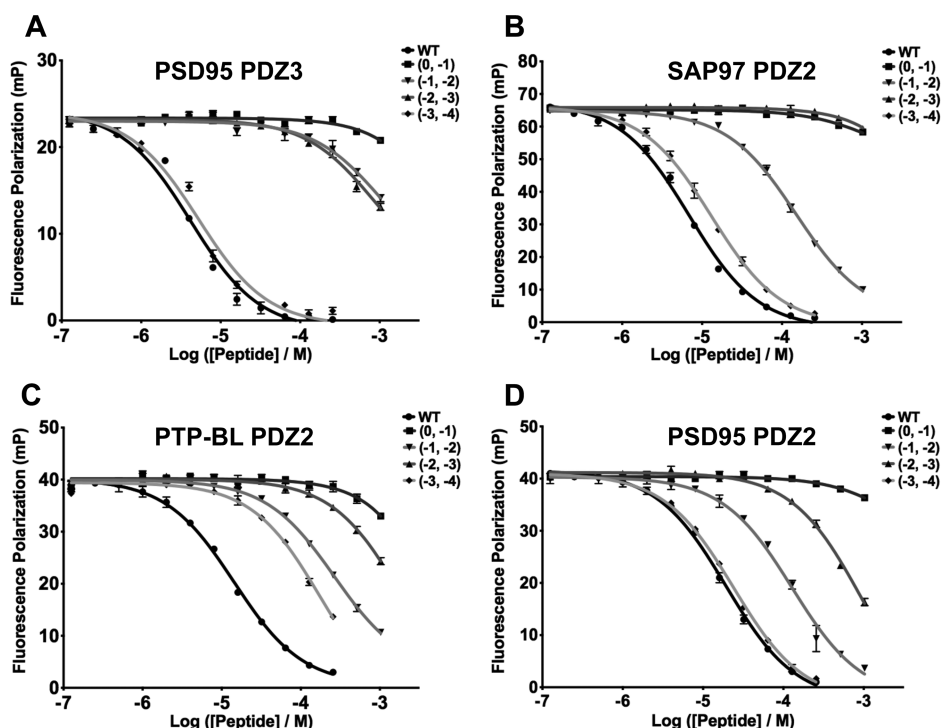
Figure 2. Fluorescence polarization binding assay of wild-type and mutated peptides. There is a clear effect of the amide-to-ester mutations in the peptide ligands except for position (−3,−4), for which a large reduction in affinity is only observed for PTP-BL PDZ2. Fluorescence polarization values are given in millipolarization units (mP) and were measured at excitation/emission wavelengths of 635/670 nm. WT is the corresponding wild-type peptide for each PDZ domain. See Table 1 for fitted K_i values.

Table 1. Equilibrium Parameters on PDZ−Peptide Interactions from Fluorescence Polarization Assays

	PSD-95 PDZ3 YKQTSV		SAP97 PDZ2 RRETQV		PTP-BL PDZ2 EQVSAV		PSD-95 PDZ2 SIESDV	
peptide mutation	K_i, μM	$\Delta\Delta G$,[a] kcal/mol	K_i μM	$\Delta\Delta G$, kcal/mol	K_i μM	$\Delta\Delta G$, kcal/mol	K_i μM	$\Delta\Delta G$, kcal/mol
wild-type	0.57 ± 0.07	−	1.5 ± 0.02	−	5.8 ± 0.2	−	6.7 ± 0.4	−
(0,−1)	>1000	>4.4	>1000	>3.8	>1000	>3.1	>1000	>3
(−1,−2)	630 ± 50	4.2 ± 0.2	45 ± 0.1	2.0 ± 0.02	120 ± 3	1.8 ± 0.04	56 ± 1.3	1.3 ± 0.1
(−2,−3)	540 ± 110	4.1 ± 0.3	>1000	>3.8	840 ± 110	3.0 ± 0.2	400 ± 40	2.4 ± 0.1
(−3,−4)	1.2 ± 0.05	0.4 ± 0.2	3.4 ± 0.2	0.48 ± 0.06	80 ± 5	1.6 ± 0.1	8.6 ± 0.7	0.15 ± 0.09

[a]The $\Delta\Delta G$ value is defined as $\Delta G^{mutant} - \Delta G^{wild-type}$.

peptide, in agreement with X-ray crystal and NMR structures.[14,51−55] A systematic approach was taken where an amide-to-ester mutation was introduced in each of the four C-terminal amide bonds in each ligand, at positions denoted (0,−1), (−1,−2), (−2,−3), and (−3,−4) (Figure 1A), resulting in 16 mutated peptides (depsipeptides) (see Methods section for details). A dansyl group was attached to the N-terminus of each peptide to allow fluorescence based binding studies. While the dansyl group may weakly interact with the PDZ domain, it should not interfere with our conclusions since we compare binding affinity and kinetics to the respective wild-type dansylated peptide to obtain $\Delta\Delta G$ values on mutation.

Synthesis of Depsipeptides. Depsipeptides are generally prepared by introduction of an α-hydroxy acid instead of the α-amino acid, however only a limited number of α-hydroxy acids are commercially available, and in biological studies using depsipeptides conservative side-chain mutations are often introduced along with the backbone mutation to accommodate the commercially available α-hydroxy acids. But for PDZ domain peptide ligands, it is well-established that side-chain mutations result in loss of affinity, particularly at the 0 and −2 positions.[17,19,21,23] Therefore, in order to get a precise

measurement of the result of an amide-to-ester mutation, it is crucial to employ α-hydroxy acids with native side chains. For the synthesis of the 16 depsipeptides, α-hydroxy acid versions of Val and Ala were commercially available, whereas corresponding versions of Ser, Thr, Asp, and Glu were prepared as inspired by Kelly and co-workers.[56] For synthesis of the α-hydroxy version of Gln see Supporting Information. For introduction of an amide-to-ester mutation in position (0,−1) (S)-(+)-hydroxy-3-methylbutyric acid was loaded onto a resin with subsequent amino acid coupling to form an ester bond using Fmoc-based SPPS. For the reminder of the depsipeptides, resins preloaded with Val were used in Boc SPPS using standard conditions, except for introduction of the α-hydroxy acid and subsequent ester formation (Figure 1B). Wild-type peptides were prepared by standard Fmoc SPPS, and a dansyl group was introduced in the N-terminus of all peptides using dansyl chloride.

Effect of Amide-to-Ester Mutations on Equilibrium Binding between Peptide and PDZ Domain. Based on X-ray crystal and NMR structures of PDZ domains with bound ligands,[14,51−55] it can be foreseen that two of the amide-to-ester mutations, at positions (0,−1) and (−2,−3), result in complete
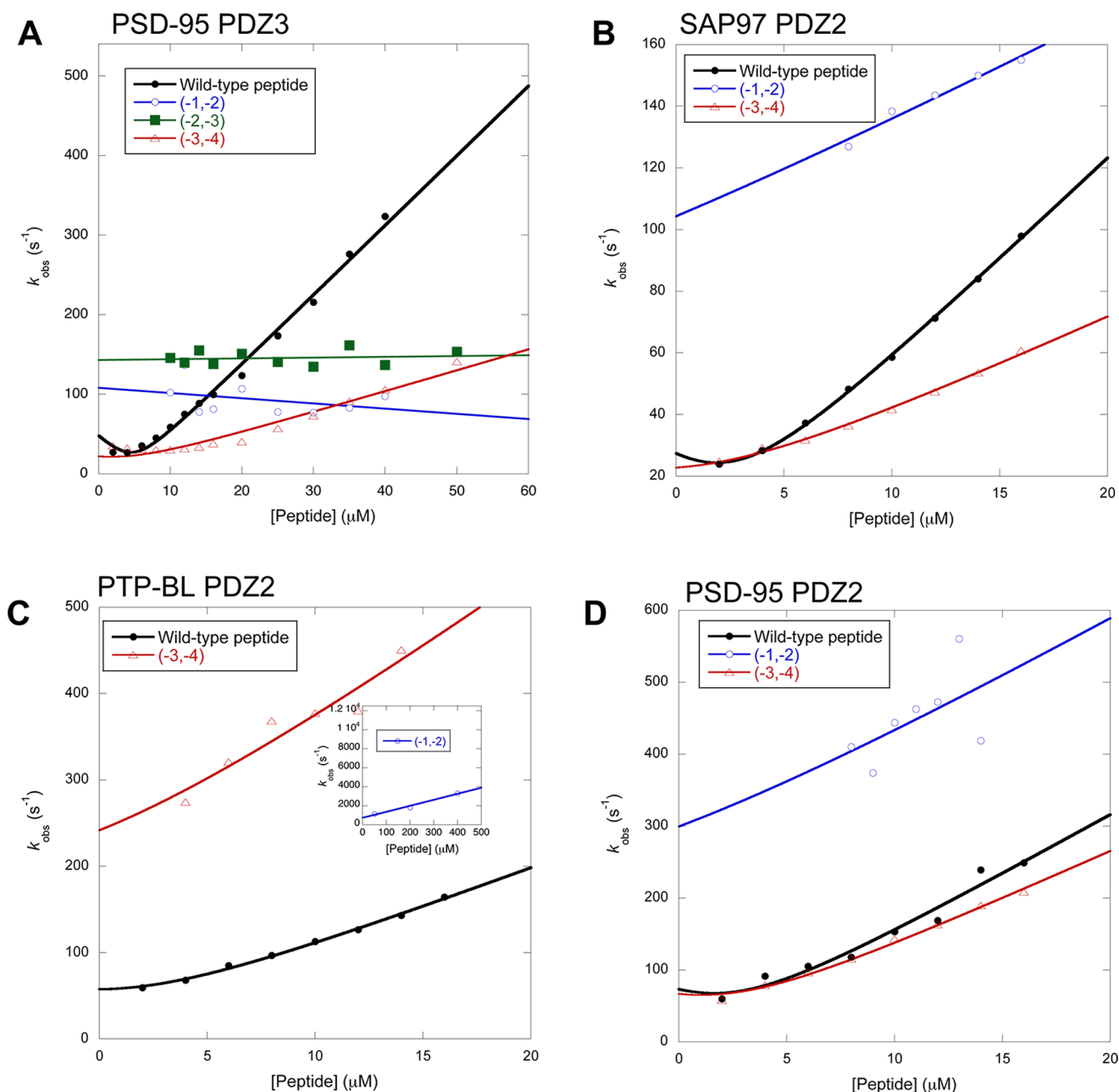
Figure 3. Binding kinetics of wild-type and amide-to-ester mutated peptides. The severe destabilization of the majority of peptide−PDZ complexes upon mutation only allowed determination of a limited set of kinetic rate constants. It is however clear that the effect is mainly in k_{off}, except for two positions for PSD-95 PDZ3, suggesting that these hydrogen bonds form early in the binding reaction. See Table 2 for fitted kinetic parameters.

removal of a hydrogen bond from the peptide NH to a carbonyl oxygen in the protein (Figure 1A). The NH groups mutated at the other two positions in the peptide (−1,−2) and (−3,−4) are not directly involved in hydrogen bonds. However, their adjacent carbonyls are engaged in hydrogen bonds with backbone NH groups in the $\beta2$-strand in the PDZ domain. The amide-to-ester mutations are expected to destabilize these interactions because the ester carbonyl is a weaker hydrogen-bond acceptor as compared to that in the amide.[24,25] First, we measured the inhibition constants for the wild-type and depsipeptides toward their respective PDZ domain in a fluorescence polarization binding assay. These experiments showed that all four PDZ domains bind to all depsipeptides with K_i values ranging from close to that for the wild-type peptide for the (−3,−4) position (1−10 μM) to between 45

μM and >1 mM for the other three positions (Figure 2, Table 1).

The fluorescence polarization experiments further demonstrated that the two mutations expected to remove a peptide−NH/protein−C═O hydrogen bond resulted in severe loss of affinity toward the protein (100- to >1000-fold) (Figure 2). In general, mutation at position (0,−1) was more deleterious compared to that at (−2,−3), and mutations at position (−1,−2) reduced the affinity relatively more than at (−3,−4). In fact, for PSD-95 PDZ2, PSD-95 PDZ3, and SAP97 PDZ2, the change in affinity was only 2-fold or less for the amide-to-ester mutation at (−3,−4), showing that this hydrogen bond to the carbonyl group in the peptide contributes relatively little to the overall PDZ-peptide affinity. Note that $\Delta\Delta G$ values for mutations at (0,−1) and (−2,−3) on the one hand cannot be

compared directly to those at $(-1,-2)$ and $(-3,-4)$ on the other, because the amide-to-ester mutation removes completely the hydrogen bond for the former but only destabilizes the hydrogen bond for the latter (Figure 1A).

Effect of Amide-to-Ester Mutation on Binding Kinetics. To understand the binding reaction in more detail, we performed stopped flow experiments for all pairs of PDZ and cognate peptides (Figure 3, Table 2). We were not able to

Table 2. Kinetic Rate Constants for PDZ–Peptide Interactions from Stopped Flow Fluorimetry

peptide mutation	PSD-95 PDZ3 YKQTSV		SAP97 PDZ2 RRETQV	
	k_{on}, $\mu M^{-1}s^{-1}$	k_{off}, s^{-1}	k_{on}, $\mu M^{-1}s^{-1}$	k_{off}, s^{-1}
wild-type	8.8 ± 0.2	3.3 ± 0.3	6.7 ± 0.1	4.9 ± 0.05
$(0,-1)$	$-^a$	$-^a$	$-^a$	$-^a$
$(-1,-2)$	0.11 ± 0.24	143 ± 8	3.8 ± 0.4	93 ± 5
$(-2,-3)$	-0.6 ± 0.6	111 ± 18	$-^a$	$-^a$
$(-3,-4)$	2.7 ± 0.2	1.9 ± 0.15	3.2 ± 0.1	8.4 ± 0.1

peptide mutation	PTP-BL PDZ2 EQVSAV		PSD-95 PDZ2 SIESDV	
	k_{on}, $\mu M^{-1}s^{-1}$	k_{off}, s^{-1}	k_{on}, $\mu M^{-1}s^{-1}$	k_{off}, s^{-1}
wild-type	9.4 ± 0.2	30 ± 1	17 ± 1	23 ± 5
$(0,-1)$	6.3 ± 0.9^b	700 ± 200^b	$-^a$	$-^a$
$(-1,-2)$	$-^a$	$-^a$	17 ± 13	250 ± 120
$(-2,-3)$	$-^a$	$-^a$	$-^a$	$-^a$
$(-3,-4)$	18 ± 3	190 ± 25	14 ± 0.4	26 ± 2

^{a}Too high k_{obs} value and/or too low kinetic amplitude to measure the parameter accurately. ^{b}Determined by temperature jump fluorimetry.

measure binding kinetics for the peptides with the amide-to-ester mutation at position $(0,-1)$. Based on the fluorescence polarization data $(K_d > 1 \text{ mM})$, a likely explanation is off-rate constants higher than 1000 s^{-1}, i.e., outside the range of the stopped flow mixer, which can measure reactions occurring after approximately 2 ms.

For mutations at position $(-3,-4)$ the kinetic experiments confirmed those from fluorescence polarization, namely that this hydrogen bond makes only a small contribution to the binding of peptide ligand. However, for both PSD-95 PDZ3 and SAP97 PDZ2, the association rate constant k_{on} decreased upon mutation in position $(-3,-4)$ suggesting that this hydrogen bond is contributing early, in the rate-limiting transition state for the binding reaction. To quantify the formation of native hydrogen bonds in the transition state of the binding reaction, we calculated $\Phi_{binding}$ values[45] (see Methods section) (Table 3). A $\Phi_{binding}$ value of zero is interpreted as no formation of the hydrogen bond in the transition state, and a value of one as a fully developed native bond. Intermediate values may be interpreted as partial formation of the hydrogen bond in the transition state, but see Fersht and Sato for caveats involving Φ analysis.[57]

At position $(-1,-2)$ we measured binding kinetics for PSD-95 PDZ2 and SAP97 PDZ2 using the stopped flow technique. For these two PDZ domains an increase in k_{off} made the major contribution to the loss of affinity, i.e., this hydrogen bond forms mainly after the rate-limiting barrier for binding, with $\Phi_{binding}$ values close to zero. Using capacitor discharge temperature jump we could also estimate a low $\Phi_{binding}$ value for PTP-BL PDZ2 at position $(-1,-2)$ (Figure 3, Tables 2 and 3).

Table 3. $\Phi_{binding}$ Values for the Amide-to-Ester Mutations in Peptide Ligands for the Binding Reaction with PDZ Domains

peptide mutation	PSD-95 PDZ3 YKQTSV		SAP97 PDZ2 RRETQV	
	$\Delta\Delta G_{K_d}$, kcal/mol	Φ	$\Delta\Delta G_{K_d}$, kcal/mol	Φ
$(0,-1)$	–	–	–	–
$(-1,-2)$	4.4 ± 0.3	0.47 ± 0.07	2.1 ± 0.1	0.15 ± 0.03
$(-2,-3)$	4.3 ± 0.3	0.49 ± 0.07	–	–
$(-3,-4)$	0.38 ± 0.08	1.8 ± 0.8	0.75 ± 0.02	0.54 ± 0.02

peptide mutation	PTP-BL PDZ2 EQVSAV		PSD-95 PDZ2 SIESDV	
	$\Delta\Delta G_{K_d}$, kcal/mol	Φ	$\Delta\Delta G_{K_d}$, kcal/mol	Φ
$(0,-1)$	–	–	–	–
$(-1,-2)$	2.1 ± 0.2	0.11 ± 0.01	1.4 ± 0.5	0.0 ± 0.3
$(-2,-3)$	–	–	–	–
$(-3,-4)$	0.7 ± 0.1	-0.55 ± 0.17	0.21 ± 0.14	–

We could also measure binding kinetics for PSD-95 PDZ3 at position $(-1,-2)$ and, unlike for the other three PDZ domains, at position $(-2,-3)$. However, instead of the linear increase of k_{obs} with peptide concentration, typical for a bimolecular interaction,[45] the k_{obs} values appeared to be constant with increasing peptide concentration (Figure 3). Importantly, fluorescence polarization data showed that the interactions between PSD-95 PDZ3 and the $(-1,-2)$ and $(-2,-3)$ depsipeptides are weak, in agreement with a very low k_{on}. Calculated from the extrapolated k_{off} (Figure 3) and K_d from fluorescence polarization (Figure 2, Table 1), the k_{on} values would be around $0.2 \ \mu M^{-1}s^{-1}$ for both peptides. This value is within the error of what we can observe directly in the stopped-flow measurements, given the experimental scatter resulting from low kinetic amplitudes and relatively high k_{obs} values. Using these numbers the $\Phi_{binding}$ values for the hydrogen bonds at positions $(-1,-2)$ and $(-2,-3)$ for the PSD-95 PDZ3– peptide interaction can be estimated to 0.5, indicating partial formation of the native hydrogen bonds in the transition state for binding. Mutation at position $(-3,-4)$ resulted in a nonclassical $\Phi_{binding}$ value of 1.8, resulting from a decrease in k_{off} as well as in k_{on}. This may be interpreted as a nonfavorable interaction in the native bound state by the $(-3,-4)$ hydrogen bond, although there are other interpretations. The effect on k_{on} is however clear suggesting that this amide makes a favorable interaction in the transition state for binding.

Effect of Amide-to-Ester Mutation on Peptide Conformational Preferences. Amide-to-ester mutations have been widely used to address backbone interactions in peptides and proteins, in particular to delineate specific hydrogen-bonding contributions, assuming that esters are structurally similar to amides.[27−32] However, internally in the peptide, the amide-to-ester mutation represents an *umpolung* of the electrostatic properties stabilizing the internal conformation of the peptide ligand. Upon amide-to-ester mutation, a hydrogen-bond donor is converted to a weak hydrogen-bond acceptor, and for the individual amino acid, this means that a favorable 1,4-intramolecular electrostatic interaction between the hydrogen in the NH group and the carbonyl oxygen is replaced by an unfavorable interaction due to two lone pairs pointing in the same direction. To get an overview of this effect on the investigated peptides, we compared computational torsional scans for wild-type and depsipeptides, and the results indicate that for $(0,-1)$, $(-1,-2)$ and $(-2,-3)$ depsipeptides,
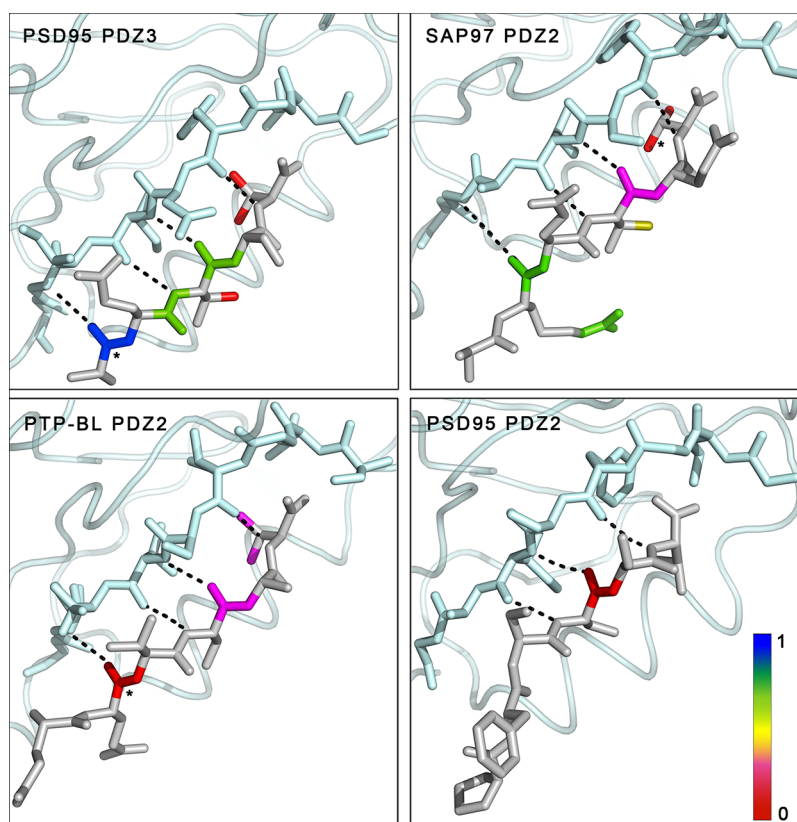
Figure 4. The degree of formation of hydrogen bonds in the transition state for binding between PDZ domains and peptides. Binding Φ values were calculated and values were mapped onto the native structures of PDZ and peptide (Protein Data Bank codes: PSD-95 PDZ3, 1BE9; SAP97 PDZ2, 2I0L; PTP-BL PDZ2, 3LNY; and PSD-95 PDZ2, 2KA9) to picture the degree of formation of hydrogen bonds. Binding Φ values for side chains from a previous study[67] were also included. The star indicates a noncanonical Φ value; blue >1, red <0. Black dots represent probed backbone−backbone hydrogen bonds.

energy minima have shifted significantly for at least one of the two torsional angles associated with the backbone ester oxygen atom relative to the corresponding dihedral in the wild-type peptide (Figure S1). In most cases, the relative energy of the depsipeptide exceeds that of the wild-type peptide in vicinity of the dihedral angle extracted from the bound ligand indicating that there is a conformational energy penalty associated with adopting a conformation similar to that observed for the wild-type peptide bound in the PSD-95 PDZ3[14] X-ray crystal structure. To quantify the effect, we compared the conformational energy preferences of the peptide fragment, Val−CO−CH_3 to that of its α-hydroxy analogue representing the (0,−1) depsipeptide. The fragment was chosen instead of the full peptide because it is sufficiently small in size to allow for use of more accurate quantum mechanical calculations. The results show that to assume a conformation corresponding to that of the bound wild-type peptide, the (0,−1) depsipeptide has to pay a conformational energy penalty of 1.5 kcal/mol (Figure S2). Thus, we note that conformational preferences of free versus bound peptide may contribute to the large apparent changes in binding energy upon amide-to-ester mutation. In general, it is likely that such conformational preferences affect the outcome of amide-to-ester mutations.

■ DISCUSSION

Hydrogen bonds play pivotal roles in molecular recognition.[58,59] In particular, they often serve as determinants of specificity in protein−protein interactions and enzyme−substrate binding, whereas hydrophobic interactions generally afford affinity. However, this appears to not be the case for PDZ−peptide interactions, for which a similar set of hydrogen bonds are always present between a β-strand in the PDZ domain and the linear motif of its protein ligand (Figure 1A). In sharp contrast to the role of side chains in PDZ−ligand interactions, the backbone hydrogen bonds have never been investigated. We therefore set out to quantitatively measure the contribution of these hydrogen bonds to the binding reaction by making amide-to-ester mutations[24,27] in the backbone of peptide ligands for four different PDZ domains. Intermolecular hydrogen bonds are important in many protein−ligand interactions,[59] including pathological fibril formation.[60] The strategy presented in the current paper may be extended to other systems involving binding of linear motifs, which is very common, for example, among intrinsically disordered protein regions.[61]

The large effect on the affinity upon removal or perturbation of the backbone hydrogen bonds between peptide residues 0 and −3 demonstrates their significance in terms of binding energy for the interaction with the β2-strand of the PDZ domain. However, the net energetic contribution or the genuine incremental binding energy[58] of a particular hydrogen bond in the peptide−PDZ complex is difficult to estimate. It is well-known that the net change in number of hydrogen bonds in a binding reaction is usually zero, and so the change in free energy will usually be only 0.8−1.5 kcal mol^{-1},[58] whereas the actual strength of the hydrogen bond could be higher, in particular in a hydrophobic environment.[31] In the interaction

13004

dx.doi.org/10.1021/ja402875h | J. Am. Chem. Soc. 2013, 135, 12998−13007

between wild-type peptide ligands and PDZ domains, the backbone NH groups from the peptide will form a hydrogen bond with bulk water in its free form as well as one hydrogen bond in the complex with the PDZ domain. Our amide-to-ester mutations at position $(0,-1)$ and $(-1,-2)$ probably result in net loss of a hydrogen bond: The backbone oxygen in the ester of the mutated peptide will form hydrogen bond(s) with water in its free form but likely not when bound to the PDZ domain. In addition, mutation at these positions may introduce electrostatic repulsion between the carbonyl oxygen in the PDZ and the ester oxygen in the peptide, further contributing to the destabilization of the complex. The amide-to-ester mutations at $(-1,-2)$ and $(-3,-4)$ are likely to retain the total number of hydrogen bonds (as reflected in the lower observed $\Delta\Delta G$ on mutation) and are therefore more conservative as site-directed perturbations for the calculation of $\Phi_{binding}$ values. The difference in number of hydrogen bonds relates to the difference in desolvation energy comparing a peptide and the corresponding depsipeptide. For the Phe-Phe dipeptide, the difference in desolvation energy was estimated to be in the order of 0.5 kcal/mol in favor of the depsi-dipeptide which means that it pays a lower desolvation penalty compared to the wild-type peptide.[62] Further, an unfavorable contribution from O−O repulsion will contribute to the overall free energy. This repulsion may be on the order of 0.3−0.4 kcal/mol,[62,63] but both the desolvation and the repulsion terms are complicated by the fact that the peptide binds in a shallow groove on the PDZ, with access to surrounding water.

Furthermore, our theoretical studies indicate that the amide-to-ester mutations do more than perturbing the respective hydrogen bond. Conformational factors most likely also play a role, and since the conformational energy associated with adopting the bound conformation is directly associated with the binding free energy, this contribution is important to take into account and may be significant. For example, in the case of the $(0,-1)$ depsipeptide, the theoretical conformational energy penalty assumes a magnitude comparable to the reported energy contribution of a standard hydrogen bond and is likely to contribute to the large energy loss upon mutation at this position. So far, only a few studies investigating structural consequences of amide-to-ester substitutions in peptide ligands have been reported, and so far the data suggest that differences indeed exist and that these potentially can be used advantageously to fine-tune the conformations of ligands.[64−66]

The binding Φ values of the amide-to-ester mutations that we could calculate with any confidence were low for the $(-1,-2)$ position and variable for the $(-3,-4)$ position (Figures 3 and 4, Table 3). We have previously investigated $\Phi_{binding}$ values for side chains of the peptide ligand and found that they were lower toward the C-terminus of the peptide ligand but intermediate for the side-chains at positions -2 and -4, in particular for SAP97 PDZ2 with the peptide LQRRRETQV.[67,68] In agreement with the truncation of the side-chains, the current $\Phi_{binding}$ values for the amide-to-ester mutations display a similar pattern. The combined data are thus consistent with a mechanism where few native interactions are formed toward the C-terminus of the peptide ligand in the rate-limiting transition state for binding. Partially formed native interactions are found around N-terminal peptide residues where we observe partial backbone interactions with β2 of the PDZ domain. But, there are also interesting individual differences among the PDZ domains, for example, for PSD-95 PDZ3, the $\Phi_{binding}$ values for amide-to-ester mutations are

clearly larger than that from truncation of the Thr side-chain ($\Phi_{binding} = 0$) at the same peptide position, where the whole destabilization on mutation is due to an increase in k_{off}.[23,67] Thus, for this PDZ−peptide interaction, formation of hydrogen bonds appears to precede formation of native side-chain interactions and guide peptide binding over the rate-limiting barrier. The noncanonical $\Phi_{binding}$ value (1.8) for the $(-3,-4)$ depsipeptide results from lower k_{off} and k_{on} values. Thus, the hydrogen bond appears to guide binding by forming a stabilizing interaction in the transition state but is slightly destabilizing in the bound state. On the other hand, the $\Phi_{binding}$ value for PTP-BL PDZ2 at this position displays a negative value (-0.55) resulting from an increase in both k_{off} and k_{on}. This could be interpreted as a destabilizing interaction in the transition state and a stabilizing bond in the native complex. In PSD-95 PDZ2 this hydrogen bond is absent and in SAP97 PDZ2 it displays an intermediate $\Phi_{binding}$ value. We speculate based on these observations that the $(-3,-4)$ hydrogen bond allows for functional adaption in the PDZ family. However, unusual Φ values may have alternative explanations, such as structural changes in the free ground states.[69,70]

CONCLUSIONS

We have, to the best of our knowledge, for the first time examined the contribution of backbone hydrogen bonds in a protein−peptide interaction using the common peptide−PDZ model system as an example. Amide-to-ester bonds were systematically introduced into the peptide ligand, and strong but differential effects on binding were observed. Consistent with structural data, always three and sometimes four amide bonds had a dramatic impact on the affinity, demonstrating that they make favorable hydrogen-bond interactions in the complex. Our current model for peptide binding by PDZ domains, based on previous experiments with ultrafast mixing techniques, involves an intermediate that accumulates at very high peptide concentration ($>200\ \mu$M) and which is present before the major rate-limiting barrier for binding.[41,51] With the current data at hand, which probes the rate-limiting barrier for association, we suggest that this early intermediate contains mainly non-native interactions. During the passage over the rate-limiting barrier, a few native bonds are beginning to form, including backbone−backbone hydrogen bonds (Figure 4, Table 3). Thus, in PDZ−peptide interactions, native backbone−backbone and side chain interactions appear to form simultaneously, and they start to do so toward the N- rather than C-terminus of the peptide ligand (at least for PSD-95 PDZ3 and SAP97 PDZ2). The majority of the interactions, including the backbone hydrogen bonds, obtains fully native contacts on the downhill side of the rate-limiting barrier for all PDZ domains studied.

ASSOCIATED CONTENT

⑤ Supporting Information
Additional figures (Figure S1 and S2), Table S1 and methods (pp S4−S5). This material is available free of charge via the Internet at http://pubs.acs.org.

AUTHOR INFORMATION

Corresponding Author
Per.Jemth@imbim.uu.se; kristian.stromgaard@sund.ku.dk

Notes
The authors declare no competing financial interest.

■ REFERENCES

(1) Sheng, M.; Sala, C. *Annu. Rev. Neurosci.* **2001**, *24*, 1−29.
(2) Kim, E.; Sheng, M. *Nat. Rev. Neurosci.* **2004**, *5*, 771−781.
(3) Chi, C. N.; Bach, A.; Strømgaard, K.; Gianni, S.; Jemth, P. *BioFactors* **2012**, *38*, 338−348.
(4) Ivarsson, Y. *FEBS Lett.* **2012**, *586*, 2638−2647.
(5) Feng, W.; Zhang, M. *Nat. Rev. Neurosci.* **2009**, *10*, 87−99.
(6) Saras, J.; Heldin, C. H. *Trends Biochem. Sci.* **1996**, *21*, 455−458.
(7) Dev, K. K. *Nat. Rev. Drug Discovery* **2004**, *3*, 1047−1056.
(8) Wang, N. X.; Lee, H. J.; Zheng, J. J. *Drug News Perspect.* **2008**, *21*, 137−141.
(9) Aarts, M.; Liu, Y.; Liu, L.; Besshoh, S.; Arundine, M.; Gurd, J. W.; Wang, Y. T.; Salter, M. W.; Tymianski, M. *Science* **2002**, *298*, 846−850.
(10) Cook, D. J.; Teves, L.; Tymianski, M. *Nature* **2012**, *483*, 213−217.
(11) Hill, M. D.; Martin, R. H.; Mikulis, D.; Wong, J. H.; Silver, F. L.; Terbrugge, K. G.; Milot, G.; Clark, W. M.; Macdonald, R. L.; Kelly, M. E.; Boulton, M.; Fleetwood, I.; McDougall, C.; Gunnarsson, T.; Chow, M.; Lum, C.; Dodd, R.; Poublanc, J.; Krings, T.; Demchuk, A. M.; Goyal, M.; Anderson, R.; Bishop, J.; Garman, D.; Tymianski, M. *Lancet Neurol.* **2012**, *11*, 942−950.
(12) Bach, A.; Clausen, B. H.; Møller, M.; Vestergaard, B.; Chi, C. N.; Round, A.; Sørensen, P. L.; Nissen, K. B.; Kastrup, J. S.; Gajhede, M.; Jemth, P.; Kristensen, A. S.; Lundström, P.; Lambertsen, K. L.; Strømgaard, K. *Proc. Natl. Acad. Sci. U.S.A.* **2012**, *109*, 3317−3322.
(13) Andreasen, J. T.; Bach, A.; Gynther, M.; Nasser, A.; Mogensen, J.; Strømgaard, K.; Pickering, D. S. *Neuropharmacology* **2012**, *67*, 193−200.
(14) Doyle, D. A.; Lee, A.; Lewis, J.; Kim, E.; Sheng, M.; MacKinnon, R. *Cell* **1996**, *85*, 1067−1076.
(15) Lim, I. A.; Hall, D. D.; Hell, J. W. *J. Biol. Chem.* **2002**, *277*, 21697−21711.
(16) Hung, A. Y.; Sheng, M. *J. Biol. Chem.* **2002**, *277*, 5699−5702.
(17) Skelton, N. J.; Koehler, M. F. T.; Zobel, K.; Wong, W. L.; Yeh, S.; Pisabarro, M. T.; Yin, J. P.; Lasky, L. A.; Sidhu, S. S. *J. Biol. Chem.* **2003**, *278*, 7645−7654.
(18) Stiffler, M. A.; Chen, J. R.; Grantcharova, V. P.; Lei, Y.; Fuchs, D.; Allen, J. E.; Zaslavskaia, L. A.; MacBeath, G. *Science* **2007**, *317*, 364−369.
(19) Wiedemann, U.; Boisguerin, P.; Leben, R.; Leitner, D.; Krause, G.; Moelling, K.; Volkmer-Engert, R.; Oschkinat, H. *J. Mol. Biol.* **2004**, *343*, 703−718.
(20) Bach, A.; Chi, C. N.; Olsen, T. B.; Pedersen, S. W.; Roder, M. U.; Pang, G. F.; Clausen, R. P.; Jemth, P.; Strømgaard, K. *J. Med. Chem.* **2008**, *51*, 6450−6459.
(21) Saro, D.; Li, T.; Rupasinghe, C.; Paredes, A.; Caspers, N.; Spaller, M. R. *Biochemistry* **2007**, *46*, 6340−6352.
(22) Lee, H. J.; Zheng, J. J. *Cell Commun. Signal.* **2010**, *8*, 8.
(23) Gianni, S.; Haq, S. R.; Montemiglio, L. C.; Jürgens, M. C.; Engström, Å.; Chi, C. N.; Brunori, M.; Jemth, P. *J. Biol. Chem.* **2011**, *286*, 27167−27175.
(24) Powers, E. T.; Deechongkit, S.; Kelly, J. W. *Adv. Protein Chem.* **2006**, *72*, 39−78.
(25) Chapman, E.; Thorson, J. S.; Schultz, P. G. *J. Am. Chem. Soc.* **1997**, *119*, 7151−7152.
(26) Beligere, G. S.; Dawson, P. E. *J. Am. Chem. Soc.* **2000**, *122*, 12079−12082.
(27) Deechongkit, S.; Nguyen, H.; Powers, E. T.; Dawson, P. E.; Gruebele, M.; Kelly, J. W. *Nature* **2004**, *430*, 101−105.

(28) Deechongkit, S.; Dawson, P. E.; Kelly, J. W. *J. Am. Chem. Soc.* **2004**, *126*, 16762−16771.
(29) Scheike, J. A.; Baldauf, C.; Spengler, J.; Albericio, F.; Pisabarro, M. T.; Koksch, B. *Angew. Chem., Int. Ed. Engl.* **2007**, *46*, 7766−7769.
(30) Bunagan, M. R.; Gao, J.; Kelly, J. W.; Gai, F. *J. Am. Chem. Soc.* **2009**, *131*, 7470−7476.
(31) Gao, J.; Bosco, D. A.; Powers, E. T.; Kelly, J. W. *Nat. Struct. Mol. Biol.* **2009**, *16*, 684−690.
(32) Cupido, T.; Spengler, J.; Ruiz-Rodriguez, J.; Adan, J.; Mitjans, F.; Piulats, J.; Albericio, F. *Angew. Chem., Int. Ed. Engl.* **2010**, *49*, 2732−2737.
(33) Gordon, D. J.; Meredith, S. C. *Biochemistry* **2003**, *42*, 475−485.
(34) Bramson, H. N.; Thomas, N. E.; Kaiser, E. T. *J. Biol. Chem.* **1985**, *260*, 15452−15457.
(35) Lu, W.; Randal, M.; Kossiakoff, A.; Kent, S. B. H. *Chem. Biol.* **1999**, *6*, 419−427.
(36) Coombs, G. S.; Rao, M. S.; Olson, A. J.; Dawson, P. E.; Madison, E. L. *J. Biol. Chem.* **1999**, *274*, 24074−24079.
(37) Blum, A. P.; Lester, H. A.; Dougherty, D. A. *Proc. Natl. Acad. Sci. U.S.A.* **2010**, *107*, 13206−13211.
(38) Tavares Xda, S.; Blum, A. P.; Nakamura, D. T.; Puskar, N. L.; Shanata, J. A.; Lester, H. A.; Dougherty, D. A. *J. Am. Chem. Soc.* **2012**, *134*, 11474−11480.
(39) Chi, C. N.; Gianni, S.; Calosci, N.; Travaglini-Allocatelli, C.; Engström, Å.; Jemth, P. *FEBS Lett.* **2007**, *581*, 1109−1113.
(40) Chi, C. N.; Engström, Å.; Gianni, S.; Larsson, M.; Jemth, P. *J. Biol. Chem.* **2006**, *281*, 36811−36818.
(41) Chi, C. N.; Bach, A.; Engström, Å.; Wang, H.; Strømgaard, K.; Gianni, S.; Jemth, P. *Biochemistry* **2009**, *48*, 7089−97.
(42) Gianni, S.; Calosci, N.; Aelen, J. M.; Vuister, G. W.; Brunori, M.; Travaglini-Allocatelli, C. *Protein Eng. Des. Sel.* **2005**, *18*, 389−395.
(43) Nikolovska-Coleska, Z.; Wang, R.; Fang, X.; Pan, H.; Tomita, Y.; Li, P.; Roller, P. P.; Krajewski, K.; Saito, N. G.; Stuckey, J. A.; Wang, S. *Anal. Biochem.* **2004**, *332*, 261−273.
(44) Malatesta, F. *Biophys. Chem.* **2005**, *116*, 251−256.
(45) Schreiber, G.; Haran, G.; Zhou, H. X. *Chem. Rev.* **2009**, *109*, 839−860.
(46) Banks, J. L.; Beard, H. S.; Cao, Y.; Cho, A. E.; Damm, W.; Farid, R.; Felts, A. K.; Halgren, T. A.; Mainz, D. T.; Maple, J. R.; Murphy, R.; Philipp, D. M.; Repasky, M. P.; Zhang, L. Y.; Berne, B. J.; Friesner, R. A.; Gallicchio, E.; Levy, R. M. *J. Comput. Chem.* **2005**, *26*, 1752−1780.
(47) Qiu, D.; Shenkin, P. S.; Hollinger, F. P.; Still, W. C. *J. Phys. Chem. A* **1997**, *101*, 3005−3014.
(48) Becke, A. D. *J. Chem. Phys.* **1993**, 98.
(49) Stephens, P. J.; Devlin, F. J.; Chabalowski, C. F.; Frisch, M. J. *J. Phys. Chem.* **1994**, *98*, 11623−11627.
(50) Tannor, D. J.; Marten, B.; Murphy, R.; Friesner, R. A.; Sitkoff, D.; Nicholls, A.; Ringnalda, M.; Goddard, W. A.; Honig, B. *J. Am. Chem. Soc.* **1994**, *116*, 11875−11882.
(51) Gianni, S.; Walma, T.; Arcovito, A.; Calosci, N.; Bellelli, A.; Engström, Å.; Travaglini-Allocatelli, C.; Brunori, M.; Jemth, P.; Vuister, G. W. *Structure* **2006**, *14*, 1801−1809.
(52) Kozlov, G.; Banville, D.; Gehring, K.; Ekiel, I. *J. Mol. Biol.* **2002**, *320*, 813−820.
(53) Wang, W.; Weng, J.; Zhang, X.; Liu, M.; Zhang, M. *J. Am. Chem. Soc.* **2009**, *131*, 787−796.
(54) Zhang, Y.; Dasgupta, J.; Ma, R. Z.; Banks, L.; Thomas, M.; Chen, X. S. *J. Virol.* **2007**, *81*, 3618−3626.
(55) Zhang, J.; Sapienza, P. J.; Ke, H.; Chang, A.; Hengel, S. R.; Wang, H.; Phillips, G. N.; Lee, A. L. *Biochemistry* **2010**, *49*, 9280−9291.
(56) Deechongkit, S.; You, S. L.; Kelly, J. W. *Org. Lett.* **2004**, *6*, 497−500.
(57) Fersht, A. R.; Sato, S. *Proc. Natl. Acad. Sci. U.S.A.* **2004**, *101*, 7976−7981.
(58) Fersht, A. R. *Trends Biochem. Sci.* **1987**, *12*, 301−304.
(59) Bourgeas, R.; Basse, M. J.; Morelli, X.; Roche, P. *PloS One* **2010**, *5*, e9598.
(60) Eisenberg, D.; Jucker, M. *Cell* **2012**, *148*, 1188−1203.

(61) Uversky, V. N.; Dunker, A. K. *Anal. Chem.* **2012**, *84*, 2096−2104.

(62) Fu, Y. W.; Gao, J. M.; Bieschke, J.; Dendle, M. A.; Kelly, J. W. *J. Am. Chem. Soc.* **2006**, *128*, 15948−15949.

(63) Gao, J. M.; Kelly, J. W. *Protein Sci.* **2008**, *17*, 1096−1101.

(64) Cupido, T.; Spengler, J.; Ruiz-Rodriguez, J.; Adan, J.; Mitjans, F.; Piulats, J.; Albericio, F. *Ang. Chem. Int. Ed. Engl.* **2010**, *49*, 2732−2737.

(65) Siodlak, D.; Janicki, A. *J. Pept. Sci.* **2010**, *16*, 126−135.

(66) Choudhary, A.; Raines, R. T. *ChemBioChem* **2011**, *12*, 1801−1807.

(67) Haq, S. R.; Chi, C. N.; Bach, A.; Dogan, J.; Engström, Å.; Hultqvist, G.; Karlsson, A.; Lundström, P.; Montemiglio, L. C.; Strømgaard, K.; Gianni, S.; Jemth, P. *J. Am. Chem. Soc.* **2012**, *134*, 599−605.

(68) Karlsson, O. A.; Chi, C. N.; Engström, Å.; Jemth, P. *J. Mol. Biol.* **2012**, *417*, 253−261.

(69) Cho, J. H.; Raleigh, D. P. *J. Am. Chem. Soc.* **2006**, *128*, 16492−16493.

(70) Merlo, C.; Dill, K. A.; Weikl, T. R. *Proc. Natl. Acad. Sci. U.S.A.* **2005**, *102*, 10171−10175.